

Petrogenesis of calc-alkaline andesite from Rishiri volcano, northern Hokkaido

*Hajime Taniuchi¹, Takeshi Kuritani², Mitsuhiro Nakagawa²

1. Department of Natural History Science, Graduate School of Science, Hokkaido University, 2. Department of Natural History Science, Faculty of Science, Hokkaido University

1. Introduction

Volcanic rocks can provide useful information on the growth of the crust and the temporary change of the composition and thermal structure of the mantle beneath the volcano. Rishiri volcano is located in northern Hokkaido where no other active volcano is present. Therefore, it is a suitable target to elucidate the petrological evolution of a single volcano (Ishizuka and Nakagawa, 1999). Calc-alkaline andesite is a typical rock series in many island arcs and the composition is similar to the average composition of the continental crust. In Rishiri volcano, calc-alkaline andesite is a dominant rock type during a climactic volcanic stage. To understand the petrological evolution of the volcano, it is necessary to clarify the magmatic process of the calc-alkaline andesite. In this study, we have performed petrological and geochemical analysis of calc-alkaline andesite to understand the magmatic process.

2. Petrology

Whole-rock SiO₂ content of the products ranges from 58.2 wt.% to 65.3 wt.%, and they are divided into A-type (Andesite-type; SiO₂<62.5 wt.%) and D-type (Dacite-type; SiO₂>63.9 wt.%). The phenocryst assemblage of the A-type is olivine + cpx + opx + pl, and that of the D-type is cpx + opx + pl. A-type has crystal clots composed of pl ± olivine ± cpx ± opx, gabbroic xenolith and mafic inclusions. Olivine phenocrysts are anhedral and they have reaction rim of orthopyroxene. The Mg-number of the olivine core shows wide range (64-88). Clinopyroxene and orthopyroxene phenocrysts occur in all samples. Pyroxenes phenocrysts in A-type are reversely or normally zoned with wide core compositions. In contrast, pyroxenes phenocrysts in D-type only show normal zonation with narrow core composition. Plagioclase phenocryst are found in all samples. An-content of the plagioclase core in A-type (45-88) is wider than in D-type (49-59). Major and trace elements concentrations show linear trends in Harker diagrams except for Cr, Ni, Sr, Ba and Zr. Eu anomaly is found only in A-type. With increasing the SiO₂ contents, the ⁸⁷Sr/⁸⁶Sr and ²⁰⁶Pb/²⁰⁴Pb ratios tend to increase. The ¹⁴³Nd/¹⁴⁴Nd ratios of A-type is higher than those of D-type. There is no significant difference of the estimated P-T condition of the magma chamber between A-type (P=3.6-4.1 kbar, T=970-1000°C) and D-type (P=4.1 kbar, T=970-980°C) (two-pyroxene geo-thermometer and barometer; Putirka, 2008).

3. Discussion

The Petrological features suggest that the calc-alkaline andesite was produced by magma mixing between mafic and felsic magma. The basaltic endmember magma is suggested to have been heterogeneous on the basis of the observations that 1) the compositional trends of Ni and Cr are not linear in Harker diagram, 2) modal abundance of olivine phenocryst is the highest at around SiO₂=60 wt.%, 3) wide core composition of olivine and plagioclase. In contrast, there is no petrological evidence for magma mixing in D-type, so we interpret that D-type represents the felsic endmember magma. Therefore, A-type magma was produced by magma mixing between D-type (felsic endmember) magma and the heterogeneous basaltic endmember magma.

The chemical and isotopic composition of D-type (felsic endmember) are similar to those of high-SiO₂ Adakite (Martin, 2005) and they have significantly high-MgO, Cr and Ni concentration. This adakitic composition cannot be derived from any alkaline basalts at Rishiri volcano by crystallization and differentiation process. It is also difficult to explain the adakitic signature by direct melting of the crust,

because the isotopic composition of granodiorite (Kuritani et al., 2005) and gabbroic samples (included in A-type as xenolith) have significantly higher and lower $^{206}\text{Pb}/^{204}\text{Pb}$ ratios, respectively, than those of D-type samples. Therefore, the possible petrogenesis of the D-type magma is 1) the multiple processes including partial melting, differentiation and assimilation in crustal level, 2) the partial melting of middle crust and 3) the partial melting of the subducted slab.

Keywords: Calc-alkaline andesite, Magma mixing, Adakite, Rishiri Volcano

Genesis of ultra-high-Ni Ol in high-Mg andesite lava triggered by seamount subduction in the northeast Kamchatka

*Tatsuji Nishizawa¹, Hitomi Nakamura^{1,2,3}, Tatiana Churikova⁴, Boris Gordeychik⁵, Osamu Ishizuka⁶, Qing Chang², Atsushi Nakao¹, Hikaru Iwamori^{1,2}

1. Department of Earth and Planetary Sciences, Tokyo Institute of Technology, 2. Department of Solid Earth Geochemistry, Japan Agency for Marine-Earth Science and Technology, 3. Chiba Institute of Technology, ORCeNG, 4. Institute of Volcanology and Seismology, FED, RAS, 5. Institute of Experimental Mineralogy, RAS, 6. Institute of Geoscience and Geoinformation, Geological Survey of Japan, AIST

The northeast Kamchatka has undergone extremely dynamic processes, such as (1) hot asthenospheric injection around the slab edge (Yogodzinski et al., 2001), and (2) subduction of the Emperor Seamount Chain (Davaille and Lees, 2004). These processes are considered to be affecting the most active volcanism in the world (Klyuchevskoy Volcanic Group) (Dorendorf et al., 2000) and the northward shallowing of the subduction dip angle (Gorbatov et al., 1997). A monogenetic volcanic East Cone, EC (Fedorenko, 1969) is located in the forearc area ~60 km above the subducting Pacific Plate, which is supposed to be old and cold (~100 Ma, Renkin and Sclater, 1988). In this case, an volcanic zone other than forearc magmatism is expected to be formed above the slab of 100 km depth (Iwamori, 1998) induced by slab-derived fluid and the corresponding mantle melting. We found that the EC lavas exhibit primitive characteristics and show variability in rock-type including high-Mg andesite (HMA) and relatively primitive basalts in time (0.73–0.12 Ma) and (30 km x 60 km area). Olivine phenocrysts in the EC lavas also show different characteristics in each rock-type. Ultra-high-Ni olivine (Ni ~6300 ppm) was observed in HMA, which contain ~6300 ppm Ni, the highest value recorded in arc lavas to date (e.g., Straub et al., 2008). On the other hand the primitive basalt includes moderately-high-Ni olivine (Ni ~2900 ppm). These features reflect the dynamic processes in the northeast Kamchatka.

We discussed the enigmatic forearc magmatism based on the genetic conditions of the HMA, primitive basalt, ultra-high-Ni olivine, and temporal engagement of the seamount subduction. Inversion for trace element compositions involving subducting slab, slab-derived fluid, DMM-type mantle and melt, together with detailed inspection of the assemblages, compositions and zoning profiles of phenocrysts, indicate several isolated melt pockets and/or veins formed at the initial stage of crystallization in the mantle, each being derived from different degrees of pyroxenization along fluid pathways. Silica-rich fluids derived from a subducted seamount expelled beneath the forearc area and its chemical characteristics. Melting of heterogeneously veined mantle with such fluids produced the various primary melts in limited time and space.

Keywords: high-Mg andesite, high-Ni olivine, seamount subduction

Rotational deformation of a rhyolite lava flow below the Curie temperature of magnetite: Sanukayama rhyolite lava in Kozushima Island, Japan

*Kotaro Nakai¹, Kuniyuki Furukawa², Tatsuo Kanamaru³, Koji Uno¹

1. Graduate School of Education, Okayama University, 2. Faculty of Business Administration, Aichi University, 3. Department of Geosystem Sciences, College of Humanities and Sciences, Nihon University

Rhyolite lava flow often has a total thickness more than one hundred meters, which is made up mainly of grassy part (e.g. Manley and Fink, 1987; Furukawa and Kamata, 2005). A crystal-poor rhyolitic lava shows its flow front advance that lasts long time after the cessation of lava supply (Tuffen et al., 2013). Consolidated upper grassy part can passively be deformed due to the advance of the inner part, i.e. crystalline part, of rhyolite lava below the Curie temperatures of magnetic minerals. This study aims to investigate the characteristics of deformation, in particular the upper part, of rhyolite lava flow during the emplacement of the lava by means of paleomagnetism. The 50-70 ka, 150 m thick Sanukayama rhyolite lava in Kozushima Island, Japan is chosen as the site of our investigation. The lava shows its vertical section due to erosion, which enabled vertical paleomagnetic sampling up to about 80 m thickness. Paleomagnetic samples were taken from pumice, welded and non-welded breccia, and obsidian in the upper grassy part. In addition, crystalline rhyolite and tuffisite (lenticular body, Isshiki, 1982) in obsidian were sampled.

Remanent magnetization of the rhyolite samples is carried by magnetite, and therefore deformation during emplacement below 580 degrees C may be detected and shows that no rotational deformation occurred after complete consolidation of the lava.

Analysis of remanent magnetization of the lava shows deflection in remanence directions by 30 degrees two times above about 400 degrees C, which is as low as the grass transition temperatures of rhyolite. Therefore, the deflection in remanence directions is interpreted as deformation of the lava after the consolidation of the upper grassy part. Assuming the deformations as being rotation about a pole, the deformations of all the grassy part can be ascribed to rotation about a single axis between temperatures of 580 and 400 degrees C. In contrast to the case for the grassy part, the inner crystalline part and tuffisite have a single thermoremanent magnetization component, suggesting that these parts are considered to have retained high temperature enough to be unaffected, i.e. above the blocking temperatures of magnetite, at the time of deformation of the grassy part.

It is concluded that using paleomagnetic data, the grassy part of the Sanukayama rhyolite lava in Kozushima Island, which was cooled below the Curie temperature of magnetite, has been rotated by the advance of the inner part of the lava during its emplacement process. In contrast, tuffisite in the grassy part of the lava is considered to have retained high temperature locally at the time of rotation of the grassy part.

Keywords: rhyolite lava, deformation, paleomagnetism, Kozushima Island

Flow directions of Miocene pyroclastic flow deposits on the northern Kii Peninsula, Japan, inferred from AMS (anisotropy of magnetic susceptibility) measurements

*Hiroyuki Hoshi¹, Masanori Ito¹

1. Aichi University of Education

The northern part of the Kii Peninsula in central Japan was hit by a massive, widespread pyroclastic flow sometime between 15 and 14 Ma. This is based on the presence of the middle Miocene Muro pyroclastic flow deposit and its correlated deposits. To investigate the flow direction, we measured the anisotropy of magnetic susceptibility (AMS) of rock samples ($n = 350$) collected from 37 sites in these deposits. The samples are composed of rhyolitic-dacitic tuff (mostly welded). In general, the degree of anisotropy is not so high and the magnetic fabric is dominated by oblate (disk-like) shapes. Magnetic foliation and lineation data for the Muro pyroclastic flow deposit suggest that the flow direction as a whole was south to north but was not uniform on a local scale. Our AMS results imply a source pyroclastic vent (or vents) located to the south of Muro.

Keywords: AMS (anisotropy of magnetic susceptibility), pyroclastic flow deposits, flow direction, Miocene, Kii Peninsula

Possible existence of lava tube cave under Marius Hills Hole of the Moon

*Tutomu Honda¹

1. Vulcano-speleological Society

[Introduction]

The vertical pit, Marius Hills Hole (MHH), found by Haruyama has several lava layers in its cross-section (Robinson). From a mean thickness of lava flow layers in the cross section, the yield strength of the lava is estimated by using the critical condition of free Bingham fluid flow on the inclined surface. The lava tube cave height is then estimated by the critical condition of flow between the two plates or in the circular tube and compared with the actually observed height by Haruyama and Robinson. The possible cave width by using a simple beam model from the ceiling thickness is also estimated.

[Hydrodynamic model for Bingham fluid]

The lava flow model on the inclined surface with angle α is used as shown in Fig.1, where ρ is density, g is gravity, H is lava thickness and f_b yield strength of lava as Bingham fluid.

The flow critical condition of the lava is expressed as $H = nf_b / (\rho g \sin \alpha)$. The case for $n=1$, lava flows on the slope surface with a free surface, the case for $n=2$, lava flows between infinite width parallel plates and the case for $n=4$, lava flows in the circular tube (Hulme). Then, n will be between 2 and 4 for a flow in a rectangular cross sectional tube. We assumed that lava tube cave in the moon is formed as a drained flow in the circular tube or in between the parallel plates and compared with actual observation.

[Estimation of the lava yield strength and the lava tube cave height]

The depth of the MHH is 48m (Haruyama) and the cave height under MHH is 17m (Robinson), therefore the thickness of the ceiling is 31m as shown in Fig.2. The 31m thick ceiling of MHH is composed by 4 m-12 m of stratified lava layer with an average of 6 m thickness (Robinson). This average thickness $H=6$ m is used here for the lava flow critical condition in the case of $n=1$ in the Rille- A. The slope angle of 0.31 deg (Greeley), gravity $g=162 \text{ cm/s}^2$ and density $\rho=2.5 \text{ g/cm}^3$, give an estimated value of 1314 dyne/cm^2 . Consequently for $n=4$, H is 24m, for $n=2$, H is 12m. As the actual cave height is 17m, so n will be between 2 and 4 with a flow in the rectangular cross-sectional tube.

[Estimation of the lava tube cave width]

It's possible to presume the cave width sustained without the ceiling's falling down for the ceiling thickness 31m by using a simple beam model with ℓ : cave width, S : tensile strength of lava, $S=6.9 \times 10^7 \text{ dyne/cm}^2$ (Oberbeck) and the d : ceiling thickness, For a concentrated load model (Oberbeck), $\ell = (4/3) Sd / (\rho g)^{1/2} = 313 \text{ m}$. For a distributed load model (Honda), $\ell = (2Sd / \rho g)^{1/2} = 327 \text{ m}$. If the ceiling has an arch shape, the load becomes even compressive, so the cave probably becomes wider. The flow critical condition of the lava flow in the rectangular cross section tube of hollow height 17m and width 327m will be between $n=2$ and $n=4$.

[Conclusions]

The estimated value of the lava tube cave height from this consideration is in accordance with the actual measurement. It seems that a lava tube cave of rectangular cross section with height of 17m and width of 327m exists under MHH with high possibility. The hollow detection in the MHH neighborhood by gravity measurement by Sood also suggests the existence of lava tube cave. More in-depth study and future exploration are highly expected.

References:

- 1) Haruyama, J. et al (2009): Geophysical Research Letters, Vol.36, L21206, 2009.
- 2) Haruyama, J. et al (2010): 41st Lunar Planetary Science Conference, Abstract 1285, 2010.

- 3)Haruyama,J.et al(2012): Moon,Chap6,pp139-163,Springer,2012.
- 4)Robinson,M.S. et al(2012): Planetary and Space Science 69,pp18-27,2012
- 5)Hulme,G(1974).: Geophys.J.R.Astr.Soc.,Vol.39,pp361-383,1974.
- 6)Greeley,G(1971):The Moon 3(1971)pp289-314
- 7)Oberbeck,V.R. et al(1969):Modern Geology 1969, Vol. 1, pp. 75-80
- 8)Honda,T(2002): Japanese speleological society Akiyoshidai meeting p34 of proceedings in 2002
- 9)Sood,R.et al(2015): 2nd International Planetary Caves Conference (2015)
- 10)Sood,R. et al(2016): 47th Lunar and Planetary Science Conference (2016)

Keywords: Vertical pit of the Moon, Lava tube, Lava cave

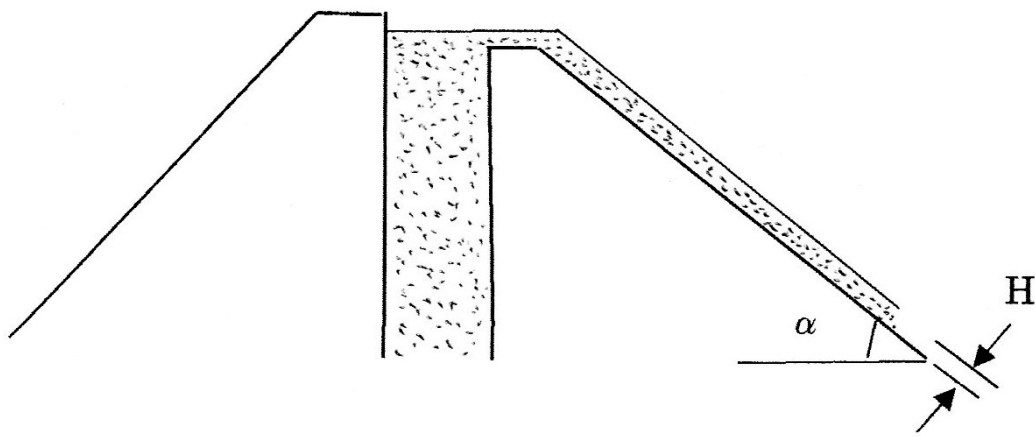


Fig.1 Critical thickness of the lava flow: $H = nf_B / (\rho g \sin \alpha)$
 $n=1$: Free surface flow, $n=2$: Flow between parallel plates,
 $n=4$: Flow in circular tube

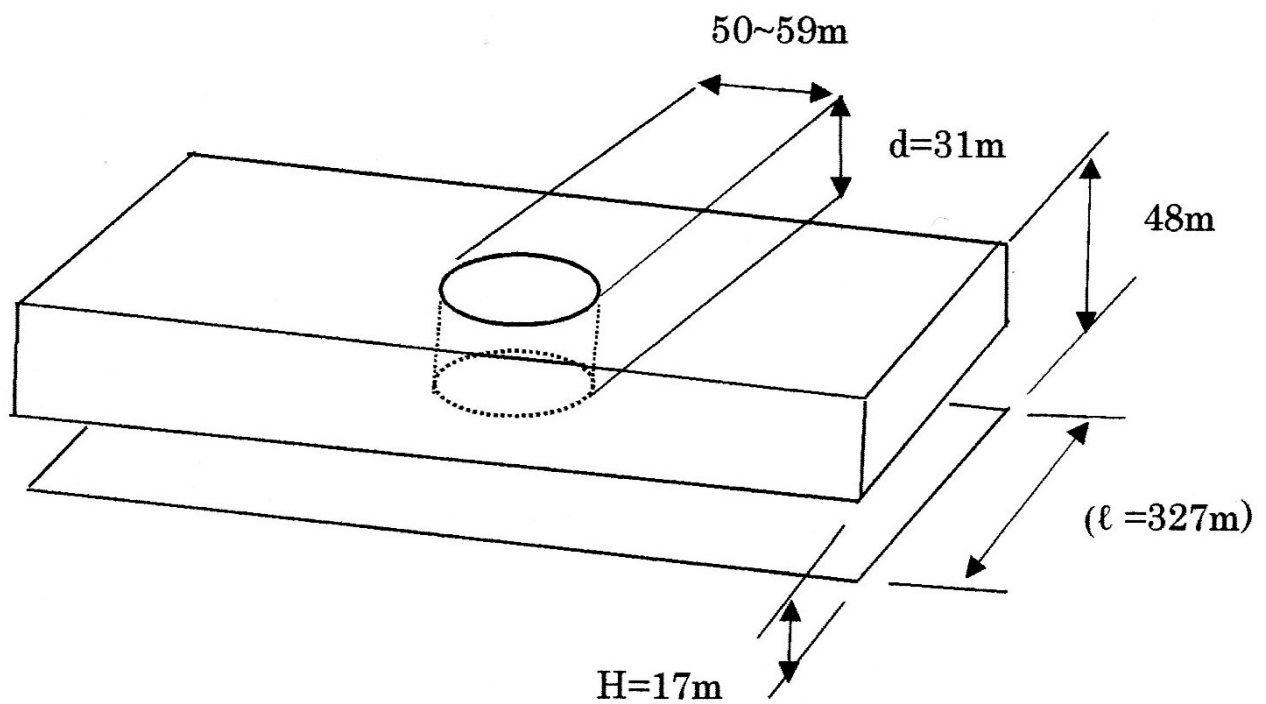


Fig.2 Schematic configuration of Marius Hills Hole

Lithofacies and Structural Development of the Sanukayama Rhyolite lava in Kozushima Island, Japan

*Kuniyuki Furukawa¹, Koji Uno², Kotaro Nakai², Tatsuo Kanamaru³

1. Aichi University, 2. Okayama University, 3. Nihon University

The Sanukayama rhyolite lava (Taniguchi, 1977; Isshiki, 1982; Goto et al., 2014) is distributed along the east coast of Kozushima Island, Japan. The ages are 70+/-5ka (Kaneoka and Suzuki, 1970), 110+/-30ka (Sugihara and Danhara, 2008), 46+/-3 and 68+/-5ka (Yokoyama et al., 2004). The lava is well exposed over 150m in height. The vertical lithofacies are mainly divided into the following three facies and transition zones between them. We describe the lithofacies and discuss the development processes.

*Pumiceous layer (Upper 40m)

Description: This layer is mainly composed of light gray- to pinkish-colored massive pumice with no obsidian. The pumice is partially brecciated into the elongated shape, and the clasts tend to be aligned to nearly vertically. The anisotropy of magnetic susceptibility (AMS) results show that the pumice was compacted horizontally rather than vertically.

Interpretation: The pumiceous layer was generated from effervescence of the upper part of the lava. The vertical oriented clasts and AMS results are consistent with the diapiric inflation (Fink and Manley, 1987).

*Obsidian layer (Middle 20m)

Description: The layer is composed of massive obsidian with nearly lack of microlites. The ductile-deformed light-colored veins, mainly with a few mm thick (exceptionally 1m thick) and a few to several meters long, are frequently observed. In the microscopic observation, the veins are composed of broken crystals and obsidian clasts.

Interpretation: In this layer, extensive vesiculation and microlite development would be prevented by higher load pressure and faster cooling, respectively, and resulted in the obsidian. The lava fracturing was ubiquitously occurred by flow-induced shear during ductile-brittle transition (Tuffen et al., 2003). The fractures were subsequently healed and deformed. Degassing would be promoted via the pervasive fractures, and the water contents of the obsidian layer would become heterogeneous.

*Crystalline rhyolite layer (Lower 50m)

Description: The layer is composed of light gray-colored crystalline rhyolite. The rhyolite is characterized by high vesicularity and flow banding. The vesicles are spherical shape with <1cm in diameter. The flow banding is defined by the ductile-deformed dark-colored veins, with 0.5mm thick and more than several cm long, and by aligned vesicles along the veins. The microscopic observation shows that the veins are composed of the microlite alignment associated with the surrounding spherulite trail.

Interpretation: The microlites would be developed on the healed fractures due to high heat retention comparing to the upper obsidian under large undercooling condition. Subsequently, the microlites acted as nucleation site of spherulite. The water rejection from the aligned spherulite consequently formed aligned vesicles.

*Pumiceous ~ Obsidian layers (<10m in thickness)

Description: The abundant discontinuous pumiceous layers with a few cm to 1m thick are intercalated in the obsidian. The layers tend to become thick into the upper part. The individual layers are linked each other by the pumiceous network.

Interpretation: The inhomogeneous water contents of the obsidian layer would be resulted in inhomogeneous effervescence. The pumiceous part are flattened by flow-induced shear and accumulated in upper part of the obsidian layer by buoyant force.

*Obsidian ~ Crystalline rhyolite layers (<10m in thickness)

Description: The crystalline rhyolite fragments are scattered within the obsidian layer. In the marginal part of the fragments, the vesicles show spherical shape, and spherulites are not broken at all. This indicates that the spherulites and vesicles were not deformed, and were developed after fragmentation.

Interpretation: The microlite development would induce increasing of viscosity. The high viscous microlite-rich layer would be fragmented by flow-induced shear. The spherulitic growth is subsequently occurred in the fragments as well as lower crystalline layer.

Keywords: rhyolite, obsidian, degassing, spherulite, Kozushima

Eruption event of Asama-Maekake volcano and the trial proposal of probabilistic event tree of its eruptive sequence

*Masaki Takahashi¹, Maya Yasui¹, Mitsuhiro Nakagawa², Minoru Takeo³

1. Department of Earth and Environmental Sciences, College of Humanities and Sciences, Nihon University, 2. Graduate School of Science, Hokkaido University, 3. Earthquake Research Institute, University of Tokyo

The eruption event of Asama-Maekake volcano consists of four types: (1) small scale single eruption (phreatic and phreato-magmatic), (2) intermediate scale single eruption (Vulcanian and Strombolian), (3) continuously eruptive stage (phreatic, phreato-magmatic, Vulcanian and Strombolian), and (4) large scale eruption (sub-Plinian or Plinian). A single eruption event occurs after a dormant interval of more than two years. In a continuously eruptive stage, eruptions continue for more than four years including an intercalating dormant stage of less than one year. A trial probabilistic event tree of eruptive sequence is proposed based on eruption events since 1527AD. The event tree begins with a magma intrusion detected by crustal deformation and volcanic earthquakes. The magma intrusion branches off to “no eruption” (67% probability) and “eruption” (33%). The “no eruption” event ends there. The “eruption” branches off to the “small scale eruption” (22%) and the “intermediate scale eruption” (78%). The “small scale eruption” ends there. The “intermediate scale eruption” branches off to the “continuously eruptive stage” (30%) and the “single eruption” (70%). The “continuously eruptive stage” ends there. The “single eruption” branches off to the intermediate scale eruption which ends there (88%) and the intermediate scale eruption which shifts to the “large scale eruption” (12%). The probability of occurrence of “large scale eruption” after a magma intrusion event is about 2%.

Keywords: Asama volcano, eruption, event tree of eruption

Relationship between the sequence of Eruptive episode C (Chuseri tephra) and the forming process of the Nakanoumi caldera, Towada volcano, NE Japan

*Noritoshi Izawa¹, Tsuyoshi Miyamoto²

1. Department of Earth Science, Graduate School of Science, Tohoku University, 2. Center for Northeast Asian Studies, Tohoku University

The Towada volcano is a double caldera volcano. The outer caldera, Towada caldera (11 km diameter), was formed 15 ka. The inner caldera, Nakanoumi caldera (3 km diameter), is a summit crater of the Goshikiwa volcano, which is a basaltic post-caldera volcano. There are still several arguments for the timing of the Nakanoumi caldera formation.

The products of Eruptive episode C (6.2 ka) consist of the following three units in ascending order: Chuseri pumice (CP), Kanegasawa pumice (KP), and Utarube ash (UA); this is one of the largest activity at post caldera stage. CP is a plinian pumice deposit, KP is stratified lithic-rich pumice fall deposits, and UA is phreatomagmatic ash deposits. Although Hayakawa (1985) considered that the Nakanoumi caldera was formed in this episode from both lithic-rich features in KP and an eruptive sequence from magmatic (CP) to phreatomagmatic (UA). Because the activity at the last stage changed to phreatomagmatic eruption for almost eruptive episodes in post-caldera stage, it is difficult to discuss the timing of caldera formation from only their evidences. So to reveal the formation processes and timing of the Nakanoumi caldera, we investigated the episode C products in detail and reconstruct the eruptive sequences.

The intermittent activities of Eruptive episode C forming plinian columns suggest that these activities are independent activities with dormancy. CP is an almost homogeneous coarse pumice deposit except for the finer part at the bottom and uppermost, and this indicates that the eruption rate of the main part was constant for at least several tens hours. Lithic amount in CP deposit is constantly low in main part, but only at the top part, the lithic fragments sharply increase. The lithic fragments in KP deposits show high contents and articulate contrast. The kinds of lithic fragments in both CP and KP are rocks derived from only shallow part forming the Goshikiwa volcano, not from deeper part. The density and chemical compositions of pumice clasts in CP and KP are constant and there are no cauliflower-like pumice clasts which show the participation of external water. The juvenile components of UA is poorly vesiculated dasitic clasts mainly and a few vesiculated particles. These features indicate that there is strong influence of external water only for UA, not so hard for CP and KP.

Macedonia *et al.* (1994) argued that the lithic fragments in tephra deposits derived from deconstruction of wall rocks by the fluid shear stress and conduit wall collapse. Roche *et al.* (2000) also argued that for small calderas like the Nakanoumi caldera, which the caldera roof aspect ratio (thickness/width) is high, high level reverse faults slice the subsiding blocks. This type caldera is considered as piecemeal type caldera by Lipman (1997). The tectonic movements by these blocks produce lithic fragments effectively and these fragments are taken by solid-gas flow in conduit. At the top of CP main part, the amount of lithic fragments increases sharply without grain size changes, it suggests that some external factors affect the increment of lithics rather than the changes of eruptive intensity. So, it is valid that the factor is the beginning of caldera subsidence. This interpretation may explain some observed facts: the lithic-rich facies on the top of CP and KP derived from the entrainment of highly fragmented rocks around the vents by faulting; intermittent activities on KP result from the several blockades between small blocks; and the apparent changes of eruptive style between KP and UA show the inflow of external water. So, we conclude that the timing of caldera subsiding was the last stage of CP and it progressed during KP and UA.

CP emitted one eruptive column with once diminished accumulating and next grew the steady one at least half a day. In the last phase of eruption, the vent collapse occurred and started the caldera formation. Next, the eruption shifted to intermittent plinian activities (KP) with progression of subsiding. External water flew in the deepened vent and contacted with solidified magma, violent phreatomagmatic eruption occurred as UA. After these activities, the deep depression was stayed behind.

Particularly in smaller calderas like the Nakanoumi caldera, collapses take place after more than half of the total volume of the eruptive materials is already erupted (Geshi *et al.*, 2014). We constrain the timing of the beginning of subsidence and eruptive volumes. The ratio of the volume before collapse (1.86km^3) and total volume (3.04km^3), 0.63, is concordant with other smaller calderas. It suggests that the forming processes of smaller calderas are unable to explain with larger one, like Druitt and Sparks (1984).

Keywords: Towada volcano, Nakanoumi caldera, Eruptive episode C, Piecemeal type caldera

Eruptive history of Asahidake Volcano, central Hokkaido: New study of the stratigraphy and eruption ages of the products.

*Kosuke Ishige¹, Mitsuhiro Nakagawa¹, Yoshihiro Ishizuka²

1. Earth and Planetary System Science Department of Natural History Sciences, Graduate School of Science, Hokkaido University, 2. National Institute of Advanced Industrial Science and Technology, Research Institute of Earthquake and Volcano Geology, Volcanic Activity Research Group

Taisetsu volcano group is part of Quaternary volcanoes in the central part of Hokkaido, Japan. Asahidake is part of Taisetsu volcano group formed after the caldera forming eruption of Ohachidaira-caldera at 34 ka (Katsui *et al*, 1979) and is considered as an active volcano with continues fumarolic activity. The activity and disaster response of Asahidake need to be evaluated through scientific research and observation because of many climbers and tourists visit the proximal area of Asahidake. The eruption history of Asahidake comprised of two eruptive stages of early and late stage (Ishige and Nakagawa, 2017). The early stage (until ca. 5 ka) is characterized by repeated magmatic eruptions formed a stratovolcano, while the late stage (since 2–3 ka) is characterized by phreatic eruptions. Eruptive history of the late stage activities was provided by Katsui et al. (1979) and Wada et al. (2001) and additional two radiometric ages by Okuno (2003). In addition, Holocene activities have been compiled in “The Active Volcano Summary” (ed. Meteorological Agency, 2013), but the supporting data has not been released. To clarify the Holocene eruption history and style of the late stage of Asahidake activity, we conducted volcanic geological survey. In addition, we reported new ¹⁴C dating of 4 samples to generate a more accurate cumulative volume step-diagram for eruptive magmas of Asahidake and clarified the characteristics of the history of phreatic eruptions activity over the past 5,000 years. Here, we also reported our evaluation to the long-term eruption history of Asahidake volcano.

New ¹⁴C dating data revealed that the magmatic eruption ages of Asahidake west lower lavas (WL) and Asahidake Summit pyroclastic rock (SU) are cal yBP 15367-15064 and 4871–4821, respectively. The eruption rate was changed from >0.2 km³ DRE/ky before 15 ka, to 1.0 km³ DRE/ky, during 15 ka to 9 ka, and 0.03 km³ DRE/ky since 9 ka to 5 ka. After 4,800 years ago, the eruption rate is considered 0 as the main eruption style became phreatic eruptions. Through detailed geological survey, we have identified two phreatic fallout depositions above SU on the proximal area. The two fallout deposits are named as Jigokudani volcanoclastic rock 1 and 2 (JD-1 and 2), in ascending order, with eruption ages are cal yBP 2845-2751 and 728-672, respectively. Eruption sequences of JD-1 were initiated by collapsed edifice producing debris avalanche which is followed by phreatic explosion. These activities formed the Jigokudani horseshoe-shaped crater. After that, lahar was effused from many small craters and fissures located in the vicinity of the opening part of the Jigokudani crater. The eruptive activity started to decrease. JD-2 eruption remarked the latest small scale phreatic eruption at North-West craters. Eruptive activity has not been frequent after the JD-1 eruption despite of the remarkable fumarolic activities. Considering the temporal change of eruptive activity, it might reasonable to infer that the activity of the Asahidake volcano has gradually decreased. However, to mitigate volcanic hazards, it should be noted that small scale of phreatic explosion and/or effusion of lahar, similar to that of JD-2 eruption, might occur near the tourism infrastructures.

Keywords: Asahidake, phreatic eruption, eruption style, eruption rate, radiocarbon dating

Omine volcano erupted just before Aso-4 pyroclastic flow

*Kousuke Shiihara¹, Toshiaki Hasenaka¹, ATSUSHI YASUDA², Natsumi Hokanishi², Yasushi Mori³

1. Graduate School of Science and Technology, Kumamoto University, 2. Earthquake Research Institute, University of Tokyo, 3. Kitakyushu Museum of Natural History and Human History

Eruption of Omine pyroclastic cone and effusion of associated Takayubaru lava occurred just before the caldera-forming Aso-4 pyroclastic eruption. Composition of Takayubaru lava and that of Aso-4 pumice are similar, but the former was flowing eruption, while the latter was explosive volcanic eruption. We examined the composition of phenocrysts and melt inclusions in Omine scoria, and compared composition with those of Aso-4 pyroclastic flow deposits.

Phenocrysts of Omine scoria is composed of plagioclase, clinopyroxene, orthopyroxene and opaque minerals, and scoria contain microphenocrysts of hornblende. Most of Plagioclase has honeycomb structure.

Whole-rock chemical composition of Takayubaru lava and that of Omine scoria are similar. Whole-rock chemical composition of Omine scoria overlap with that Aso-4 pyroclastic flow deposits in some elements, however they show distinct compositional trends in other elements such as TiO_2 , Na_2O and MgO .

The plagioclase phenocryst composition of Omine scoria shows bimodal distribution. Main peak is An_{55} and sub peak is An_{45} . Plagioclase which has sub peak has honeycomb structure and show reverse zoning. The clinopyroxene phenocryst composition shows unimodal distribution and normal zoning, but the orthopyroxene phenocryst composition shows normal and reverse zoning.

Composition of Omine melt inclusion in plagioclase, clinopyroxene and orthopyroxene are plotted in a narrow range of 68 - 70 wt.% SiO_2 , but several melt inclusion in orthopyroxene are plotted 71 -74 wt.%. Omine melt inclusions show distinct trends in major element vs. SiO_2 plots, and have less H_2O than Aso-4 melt inclusion.

Sr isotopic ratios of Aso-4 and Takayubaru lava are nearly equal. The results indicate that the magma supply system of Omine volcano was different from that of Aso-4. In addition, Omine magma chamber was injected magma of different composition.

Keywords: Omine volcano, melt inclusion, honeycomb structure

Petrological study of the 7.3 ka Kikai caldera-forming eruption (K-Ah), southern Kyushu, Japan

*Akiko Matsumoto¹, Mitsuhiro Nakagawa¹, Kyohei Kobayashi¹, Fukashi Maeno²

1. Graduate School of Science, Hokkaido University, 2. Earthquake Research Institute, University of Tokyo

Kikai caldera, located in southern Kyushu, is one of the youngest caldera volcanoes in Japan. The catastrophic caldera-forming eruption occurred ca. 7.3 ka (K-Ah eruption). It was started by a plinian eruption, followed by intraplinian pyroclastic flows (Stage 1). After that, a large ignimbrite eruption occurred, accompanied with caldera collapse (Stage 2) (Maeno & Taniguchi, 2007). This eruption was preceded by a volumetric rhyolite lava flow (Nagahama lava: NL). Although eruptive sequence of K-Ah eruption has been understood, there are few petrological studies about K-Ah eruption and therefore its magma plumbing system is still unclear. In order to understand the magma plumbing system of a large caldera-forming eruption, we carried out the petrological and geochemical investigation of K-Ah eruption including preceding activity.

The juvenile materials of K-Ah eruption are composed mainly of white pumice, and heterogeneous scoriae are also found in the upper part of Stage 2. Phenocrystic minerals are common to both juveniles of K-Ah eruption and NL, consisting of plagioclase, orthopyroxene, clinopyroxene, and magnetite. K-Ah pumice and NL have also a small amount of ilmenite. On mineral chemistry, core compositions of plagioclase in pumices show slightly wide (An₄₀₋₆₄) with a peak of An₅₅. In contrast, scoriae exhibit a clear bimodal distribution, mainly composed of An₆₄₋₉₀ with a peak of An₇₄, and a small amount of low-An plagioclase (An₄₈₋₆₂). Pyroxenes in pumice have relatively Mg-poor cores (Mg#₆₄₋₆₉ of opx and Mg#₆₈₋₇₃ of cpx) and those in scoria show higher Mg# (Mg#₆₈₋₇₃ of opx and Mg#₆₉₋₇₈ of cpx). The plagioclase and pyroxenes in pumices show normal and reverse zoning, whereas those in scoriae exhibit weak zoning. Comparing to K-Ah pumices, NL have slightly lower-An plagioclase (An₃₉₋₆₀), lower-Mg# pyroxenes (Mg#₆₄₋₆₅ of opx and Mg#₆₆₋₇₃ of cpx). On whole-rock chemistry, K-Ah pumices are rhyolitic and dacitic (SiO₂ = 70.4-73.6 wt.%), and they draw one linear trend in many Harker diagrams. Scoriae (SiO₂ = 58.1-69.0 wt.%) exhibit linear trends, which different from those of pumices. In SiO₂ vs. TiO₂ and Al₂O₃ plots, scoriae draw one linear trends, converging to dacitic end of the linear trends formed by pumices. NL are also rhyolitic (SiO₂ = 71.7-72.4 wt.%), but they are clearly different from K-Ah pumices in FeO*/MgO and Y. On Sr-Nd-Pb isotopic compositions, pumice and scoria are similar, but the former show slightly wider ranges than the latter. NL are similar to K-Ah pumices.

The heterogeneous texture of scoria and the co-existence of compositionally disequilibrium phenocrysts suggest that magma mixing is the main magmatic process in K-Ah eruption. The two distinct linear trends converging to dacitic pumice on whole-rock chemistry indicated the existence of three end-member magmas: rhyolitic, dacitic, and andesitic ones. The mixing relationship between andesitic and dacitic magmas, not rhyolitic one, as well as the co-existence of phenocrysts showing normal and reverse zoning in K-Ah pumices, suggest that there exists the silicic zoned magma chamber, in which dacitic magma stagnated beneath rhyolitic one. Andesitic magma was injected into this silicic zoned magma chamber and mixed with dacitic magma probably just before the eruption.

According to Rayleigh fractionation model, these two silicic magmas cannot be produced by simple fractionation of andesitic one. The two silicic magmas would have been generated by partial melting of crustal materials. The wide variations of isotopic chemistry of K-Ah pumices might reflect the

heterogeneity of crustal materials. The preceding activity (NL) also provided rhyolitic magma. The similarity of isotopic compositions and the difference in whole-rock chemistry suggest that NL rhyolitic magma stagnated separately from K-Ah silicic ones although their source materials are similar. In this way, the existence of multiple silicic magmas might be common in the large silicic magma system.

Keywords: Kikai caldera, large silicic magma system, multiple silicic magmas

Diversity and origin of voluminous silicic magma system

*Mitsuhiro Nakagawa¹, Akiko Matsumoto¹, Takeshi Hasegawa²

1. Division of Earth and Planetary System Science, Hokkaido University, 2. Faculty of Science, Ibaragi University

It has been widely accepted that large scaled silicic magma eruptions were caused by the mafic injections into large silicic magma storage system. In some cases, the mafic injection is considered as a trigger of eruption to produce mingled magma between the mafic and silicic magmas. On the other hand, it has been also discussed that a zoned magma chamber could be formed before the eruption by the mafic injection into the silicic magma chamber. In both cases, many previous studies have considered that the silicic magma was nearly homogeneous. However, we have recognized the possible diversity in the silicic magma from many large silicic eruptions. In case of caldera-forming eruption, such as 42 ka Shikotsu, 120 ka Kutcharo and 7.3 ka Kikai-Akahoya ones, voluminous silicic magma erupted with small amount of mafic magma. Thus, it has been concluded that mafic injection occurred just before eruption. However, there exists possible diversity of the silicic magma. The silicic magma shows compositional variations, ranging from rhyolite to dacite. In addition, many major and trace elements and isotope ratios exhibit single linear trend in SiO₂ variation diagrams. It should be noted that these linear trends do not continue to coexisted mafic magma, ranging from dacite to basaltic andesite. Thus, it can be concluded that mafic magma(s) injected into the silicic magma, which showed distinct, compositional variations. Phenocrystic minerals in the silicic magma can be compositionally distinguished from those derived from the mafic magma. These minerals, such as plagioclase and pyroxenes, show relatively wide variations. In addition, normally and reversely zoned phenocrysts coexist in a single silicic sample. These and linear trends in SiO₂ variation diagrams indicate that the silicic magma is mixing products between two silicic end-member magmas such as rhyolitic and dacitic ones. Considering isotope ratios of the silicic magma, these two end-member magmas were derived from distinct source materials. In addition, these silicic magmas could not be produced by simple differentiation processes from the mafic magmas. Thus, it can be assumed that the silicic magmas could be formed by crustal melting. Although crustal materials are usually heterogeneous, there should exist considerable difference in the region of crustal melting to produce contrasted two silicic end-member magmas. Analysis of compositional zoning profiles of phenocrystic minerals suggests that mixing between silicic magmas had occurred several hundred years before eruption. The mixing could form a zoned, large, silicic magma chamber, in which mafic magma injected just before eruption. On the other hand, eruptions of VEI=5 class, such as AD 1640 Hokkaido-Komagatake and AD 1667 Tarumai ones, also show small but possible compositional variations of the silicic magma, dacitic one. However, the variations are smaller than those in caldera-forming eruptions (VEI=7). This might correspond to the difference in volume of the region of the crustal melting to form silicic magma.

Keywords: silicic magma, magma diversity, rhyolite, caldera-forming eruption, crustal melting

Strategy for the long-term prediction of large scale volcanic eruptions

*Atsushi Toramaru¹, Shunsuke Yamashita

1. Department of Earth and Planetary Sciences, Faculty of Sciences, Kyushu University

It is important to understand what factors control when and how much large the next eruption occurs. In the case of relatively large scale eruptions exceeding VEI 4, the eruption is triggered by the overpressure due to the crystallization-induced vesiculation or the magma supply from below. In this talk, we propose the methodology for the long-term prediction of such large scale eruptions, which is controlled by the magma supply from below.

The historical eruptions of Sakurajima volcano, Bunmei, Anei, and Taisho, and Showa eruptions, provide the luckiest cases to investigate the long term behavior of large scale volcanic eruption because the volume of erupted material and eruption ages are exactly determined due to the best exposure of lavas and available documents. Thus, as the summary of geological studies, we have the precise diagram of cumulative volume versus time (so called "step diagram" frequently used in Japanese community). In addition, rich petrological data also show that at least two magmas mixed during the eruption intervals to shift the erupted compositions to mafic through 500 years, suggesting that two magma reservoirs, the upper felsic and the lower mafic reservoirs, exist as the stationary plumbing system beneath the Sakurajima volcano. Our recent CSD (Crystal Size Distribution) study for two types of plagioclase phenocrysts originated from these two endmember magma reservoirs reveals that the crystallization condition including nucleation, growth and settling of crystals in the upper felsic reservoir is nearly constant through the last 500 years, whereas in the lower mafic magma reservoir the supply rate from the mantle increases with time through the last 500 years. The advantage of CSD method allows us to quantitatively evaluate the supply rate of magmas from the mantle. Thus, applying the CSD method to historical eruptions, Sakurajima volcano, we can draw the curve of supply rate on the step diagram. As a result, it is found that the CSD derived-supply rate well explains the eruption times for the past eruptions. In addition, by extending the curve of supply rate to the future time and finding a point of intersection with the cumulative volume curve, we can predict when the next eruption takes place. To obtain a reliable result, we have to improve the estimation of supply rate from CSD data and examine the assumptions such as constant crystal growth rate in the CSD method.

Keywords: long-term prediction, large scale volcanic eruption, cumulative volume curve, CSD (Crystal Size Distribution)

Experimental constraints on pre-eruptive P-T conditions of Aso-4 silicic magma

*Masashi Ushioda¹, Isoji MIYAGI¹, Toshihiro Suzuki², Eiichi Takahashi²

1. Geological Survey of Japan, The National Institute of Advanced Industrial Science and Technology, 2. Department of Earth and Planetary Sciences, School of Science, Tokyo Institute of Technology

Aso-4 is the largest and recent caldera forming eruption (>600 km³) in the Aso volcano. In order to forecast future eruptions, understanding the magmatic process of past eruptions was very important. Determining the physical and chemical conditions (P, T, X_{H₂O}, fO₂) in the magma chamber enables us to constrain trends of crystal differentiation and compare the data with geophysical observations. Kaneko et al.(2007) carried out petrological analyses for Aso-4 products systematically and discussed the conditions of magma chamber. However, pressure of the pre-eruptive conditions, which is an important parameter for the comparison to various observations, for Aso-4 products was not determined by petrological study. In this study, the purpose was determination of pre-eruptive conditions (P, T, X_{H₂O}, fO₂) of Aso-4 silicic magma chamber. Reproduction of phenocryst assemblage and compositions of Aso-4A pumice (KJ5665: Hoshizumi, personal communication), which had the most silicic composition and was considered as the felsic end member, was carried out using high-P and high-T experiments.

KJ5665 pumice had plagioclase, orthopyroxene, magnetite, and ilmenite and trace of hornblende phenocrysts. All frequent distributions of core compositions for these phenocrysts were unimodal. Core compositions of plagioclase and orthopyroxene ranged from An₃₀ and Mg#72 to An₅₀ and Mg#75#, respectively. Temperature and fO₂ were 870~880 °C and FMQ+2, respectively, estimated by thermometer and oxygen barometer using equilibrium between magnetite and ilmenite (Lepage 2003; Andersen and Lindsley 1985). Three hydrous glasses (2.0 to 6.0 wt.% H₂O) were synthesized using the powder of KJ5665 for starting materials of high-P and high-T experiments. Melting experiments were performed in temperatures between 810 and 930 °C at 200, 400, and 700 MPa under NNO-buffered condition using IHPVs (SMC8600 and HARM200 installed at Tokyo Institute of Technology and Geological Survey of Japan, AIST, respectively). Plagioclase, orthopyroxene and/or K-feldspar crystallized with small amount of Fe-Ti oxides in the lower H₂O content of run products, while orthopyroxene did not crystallize and biotite crystallized in the higher H₂O content of run products. At 200 MPa and 900 °C and under low H₂O content (~2wt.%) of run products, plagioclase and orthopyroxene which compositions fell within the range of that of phenocrysts crystallized. In the experiments, hornblende which existed rarely as phenocrysts in the KJ5665 pumice did not crystallize. Origin of hornblende phenocrysts need to be carefully considered using various petrological features.

Acknowledgment

This study was supported by the Secretariat of the Nuclear Regulation Authority, Japan.

Keywords: high pressure and high temperature experiments, Aso-4, hydrous melting experiments, magma chamber

Collapse mechanism of small calderas: a case study of the Ohachidaira caldera, Hokkaido, Japan

*Yuki Yasuda¹, Keiko Suzuki-Kamata¹

1. Graduate School of Science, Kobe University

In order to elucidate the collapse mechanism of small calderas, we have reconstructed the Ohachidaira caldera-forming eruption and revealed componentry of lithic fragments from the proximal products of the eruption to determine the conduit evolution. The proximal products consist of five units, from base to top: pumice and scoria fall (SK-A), climactic ignimbrite (SK-B), lithic breccia (SK-C), scoria fall (SK-D), and minor ignimbrite (SK-E). A thin fine-ash layer caps SK-C lithic breccia and is overlain by SK-D scoria fall, indicating a short hiatus in explosive activity after ejection of the lithic breccia. All units consist of dacitic pumices, andesitic scorias, and banded pumices as juvenile components. During the eruption, andesitic magma ascended alongside the conduit wall while dacitic magma ascended near the conduit center, since (1) plutonic lithic fragments are coated with scoria rather than pumice indicating that conduit and/or magma chamber walls composed of plutonic rocks attached to andesitic magma, and (2) the juvenile components in SK-A change laterally outward from scoria-rich to pumice-rich, suggesting that scoria clasts ascending alongside the conduit wall were thrown to lower heights and fell on closer to the vent while pumice clasts ascending near the conduit center reached greater heights and were transported farther. The plutonic lithic content is minor in SK-A (0%) and the lower part of SK-B (2%), and increases rapidly in the middle part of SK-B (50%) suggesting a collapse of the roof of the magma chamber. It then decreases gradually in the upper part of SK-B (26%) and decreases sharply in SK-C (2%), which probably means that the collapse propagated upwards. We postulate that SK-C lithic breccia marks conduit collapse that produced abundant lithic fragments, choked the conduit, and stopped the eruption. This hypothesis is further supported by the vertical variation of the volume ratio of pumice to scoria clasts in SK-C.

Keywords: small caldera, collapse mechanism, Ohachidaira, lithic componentry, plutonic rock

Characteristics of a plinian eruption producing caldera-collapse: an example of the 40-ka Shikotsu Pyroclastic Fall Deposit, Hokkaido, Japan

*Takahiro Yamamoto¹, Mitsuhiro Nakagawa²

1. Geological Survey of Japan, AIST, 2. Department of Natural History of Science, Faculty of Science, Hokkaido University

By the collapse caldera formation, there are many examples to begin with a plinian eruption prior to a large-scale pyroclastic flow eruption.

Then what is the plinian eruption not to cause that a collapse caldera is raised different in? For this problem solution, we carried out field study for the plinian pyroclastic fall deposit (Spfa1) of the Shikotsu caldera forming eruption approximately 40 ka it was the model example of the caldera collapse and particle size analysis of the deposits. Spfa1 holds a distribution main axis in the ESE direction from Shikotsu caldera and can be traced for 180 km to Cape Erimo. And its magma volume is 40 to 48 km³ DRE. The significant characteristic of Spfa1 is that the particle size distribution of the pumice particle is different from the lower part at the upper part. Thus, the upper part shows the distribution of double modes whereas the pumice particle is lognormality distribution of the single mode at the lower part. When the upper atmosphere of November in Sapporo that the wind velocity has a big are assumed, the heights of eruption-columns are 30 to 20 km and 15 to 10 for the coarse and fine modes in the upper part, respectively.

In addition, the mass ratio of the coarse mode grains is around 70 wt% along the distribution main axis, but it decreases to 30 wt% at 25km north perpendicular to the main axis. This means that the sources of both modes existed in the place of the geographically remote independence. In other words, Spfa1 which caused the caldera-collapse was a product of coincided plural plinian eruptions, and it is thought that this eruption was different from the eruption from the normal single source in beginning of eruption.

Keywords: Shikotsu caldera, plinian eruption

Re-examination of the sequence of the Early Pleistocene Shirakawa ignimbrites and their identifications in distal areas in Northeast Japan

*Takehiko Suzuki¹, Masanori Murata², Kiyohide Mizuno³, Takeshi Ishihara³

1. Faculty of Urban Environmental Sciences, Tokyo Metropolitan University, 2. University Education Center, Tokyo Metropolitan University, 3. National Institute of Advanced Industrial Science and Technology

The Aizu volcanic region located in NE Japan is one of the Quaternary volcanic clusters resulting from the subduction of the oceanic Pacific Plate beneath the North American Plate. This volcanic region is characterised by Early Pleistocene large Shirakawa ignimbrites resulting from repeated caldera-forming eruptions and has been examined by several previous studies that established the eruptive sequence, the correlations of proximal ignimbrites with distal fall-out tephra and the eruptive history. However, the proximal sequence of ignimbrites proposed by previous studies is inconsistent with that of distal fall-out tephra, suggesting the necessity to re-examine the sequence. We present a revised stratigraphical framework of the ignimbrites included in the Nanaorezaka Formation exposed in the West Hills of the Aizu Basin, together with their petrographic description and correlations with distal fall-out tephra. From the glass chemistries and refractive indices of glass shards and phenocrysts, we identified six Early Pleistocene ignimbrites: in ascending order, the Kumado, Akai, Ashino, Nishigo, Kachikata and Ten-ei ignimbrites. In addition, the vitric widespread Kurokawa Tephra originated from a distant volcano. Four distal fall-out tephra associated with four ignimbrites (Kumado, Akai, Ashino and Kachikata) are distributed broadly in the Kanto and Niigata regions. Each combination of both the proximal and distal tephra was labelled Sr-Kmd, Sr-Aki-Kd18, Sr-Asn-Kd8 and Sr-Kc-U8, respectively. We re-examined their ages considering the stratigraphic positions of distal tephra identified in the Kanto region where calcareous nanofossil biostratigraphic and magneto-stratigraphic frameworks were available and many radiometric ages have been determined: Sr-Kmd (1.542–1.504 Ma), KK (1.533–1.485 Ma), Sr-Aki-Kd18 (1.522–1.460 Ma), Sr-Asn-Kd8 (1.219 Ma) and Sr-Kc-U8 (0.922–0.910 Ma). In addition, we estimated the volume of each fall-out tephra for Sr-Kmd, Sr-Aki-Kd18, Sr-Asn-Kd8 and Sr-Kc-U8 to be approximately 23 km³. It is concluded that the total volume of each eruptive event, except the Ten-ei eruption, ranges between 38 km³ and 173 km³. This indicates that these eruptions can be classified as VEI 6–7. The total volume of the Shirakawa ignimbrite and its associated fall-out tephra is 498 km³ (DRE: 199 km³). In addition, we estimated the eruption rate of the tephra associated with caldera-forming eruptions during the period from the Sr-Kmd to Sr-Kc-U8 eruptions to be 0.3 km³/kyr in DRE, an average value for the Quaternary volcanoes in the area of the Japanese Islands. The four repose periods between the successive eruptions were variable, ranging from approximately 0.3 My to less than 0.08 My.

Keywords: Shirakawa ignimbrites, Early Pleistocene, Northeast Japan, caldera forming-eruption, widespread tephra

Distribution and eruptive volume estimation of Ito, Hachinohe and Aso4 pyroclastic flow deposits

*Shinji Takarada¹, Takashi Kudo¹, Nobuo Geshi¹, Hideo Hoshizumi¹

1. Geological Survey of Japan, National Institute of Advanced Industrial Science and Technology

Estimation of distribution and eruptive volume of large to middle-scale pyroclastic flows are important for evaluation of affected area and emplacement processes of pyroclastic flows. Distributions and eruptive volumes just after the eruption were estimated at Ito pyroclastic flow deposit derived from Aira caldera (30ka), Hachinohe pyroclastic flow deposit derived from Towada caldera (15ka) and Aso4 pyroclastic flow deposit derived from Aso caldera (90ka). The eruptive volumes of tephra falls derived from pyroclastic flows (co-ignimbrite ash) are not included for the estimation.

The distributions of pyroclastic flow deposits just after the eruption were made by the following method.

(1) made current distributions of pyroclastic flow deposits using geological maps, and published research papers, (2) made upper and lower elevations and thickness point datasets using boring (drilling) data (eg. Kunijian and Geo-Station), published papers and geological maps, (3) convert deposit thickness into non-welded from welded part (eg. 1000kg/m³ of non-welded, 1700kg/m³ of weakly welded, 2000kg/m³ of highly welded at Ito pyroclastic flow deposit), and (4) estimate distribution of submarine area with the consideration of sea-level at the time of eruption (Ito: -100m, Aso4: -50m). For example, the energy cone simulations were used to estimate the maximum travel distances in the sea area for Ito pyroclastic flow. The energy cone parameters of Ito pyroclastic flows were H/L=0.005-0.014 and column collapse height=1050-1200m. The eruptive volume were estimated by the following method. (1) made 5km or 1km mesh data, (2) calculate the distribution area of pyroclastic flow deposit in each mesh, (3) calculate maximum, average and minimum point thickness datasets in each mesh, (4) If no point data were available in the mesh, the Kriging method were used to estimate the thickness value in the mesh, and (5) the total volume were estimated from the sum of multiply the area by the thickness data of each mesh (maximum, average and minimum cases).

The estimated eruptive volumes of Ito pyroclastic flow with 1km mesh were 325km³(max), 200km³(ave) and 130km³(min) in DRE. The estimated volumes of outflow deposit (except the within the caldera deposit) were 250km³(max), 125km³(ave) and 50km³(min) in DRE. The estimated volumes of Hachinohe pyroclastic flow (outflow deposit) with 5km mesh were 27km³(max), 20km³(ave) and 13km³(min) in DRE. The estimated volumes of Aso4 pyroclastic flow with 5km mesh were 530km³(max), 370km³(ave) and 200km³(min) in DRE. The estimated volumes of outflow deposit were 400km³(max), 270km³(ave) and 140km³(min) in DRE. The thickness of the point data sets was reduced due to erosions; therefore, the reliable eruptive volumes of pyroclastic flows were considered between maximum and average estimations. The more precise estimation of original surface and basal topography of the pyroclastic flow deposits and evaluation of distribution in the sea area are the important key factors for the estimation of eruptive volume of large-scale pyroclastic flow deposits (The above estimated volumes are provisional; the values may change due to further studies).

Keywords: Pyroclastic flow, Distribution, Eruptive Volume, Ito, Hatchnohe, Aso4